

Discovery of new mitorubrin derivatives from *Hypoxylon fulvo-sulphureum* sp. nov. (Ascomycota, Xylariales)

Esteban Benjamin Sir · Eric Kuhnert · Frank Surup · Kevin D. Hyde · Marc Stadler

Received: 30 December 2014 / Revised: 30 January 2015 / Accepted: 10 February 2015
© German Mycological Society and Springer-Verlag Berlin Heidelberg 2015

Abstract A specimen of the *Hypoxylon rubiginosum* complex featuring unusual bicoloured stromata was collected in northern Thailand and examined by means of classical morphological methodology, complemented by studies of its secondary metabolites using high performance liquid chromatography coupled with diode array and electrospray mass spectrometric detection (HPLC-DAD/MS), and molecular phylogenetic analysis of its ITS and partial beta-tubulin DNA sequences. In addition, the ultrastructure of its ascospores was examined by SEM. The chemotaxonomic studies revealed the presence of two putatively unknown, apparently specific azaphilone pigments in the stromata. These metabolites were consequently isolated to purity by preparative HPLC and identified by means of nuclear magnetic resonance spectroscopy and high resolution mass spectrometry as the novel natural products, (+)-6''-hydroxymitorubrinol acetate (**1**) and (+)-6''-hydroxymitorubrinol (**3**).

Keywords Azaphilones · Hypoxylon · Molecular phylogeny · Secondary metabolites · Taxonomy · Xylariales

Introduction

Hypoxylon Bull. is one of the largest genera of the Xylariaceae (Ascomycota) that can be assigned to the informal “subfamily” Hypoxyloideae (Stadler et al. 2013). Stromata of *Hypoxylon* mostly develop on decaying wood, and their vegetative states are frequently encountered as endophytes (Rogers 2000). Since the monograph of *Hypoxylon* by Ju and Rogers (1996), chemotaxonomic characteristics, such as surface colours and KOH-extractable stromatal pigments are considered to be important for species discrimination. However, similar pigment colours may either be due to the presence of the same or similar metabolites, or the colours may be derived from entirely unrelated secondary metabolites (Stadler and Fournier 2006). The diversity and complexity of secondary metabolites in this genus has been studied and demonstrated in several studies based on modern analytical techniques. By means of high performance liquid chromatography (HPLC) many new secondary metabolites were found from the stromata of Hypoxyloideae; for example, the daldinins (Quang et al. 2004a), macrocarpones (Mühlbauer et al. 2002), rubiginosins (Quang et al. 2004b), and cohaerins (Surup et al. 2013). Moreover, Quang et al. (2006), Fournier et al. (2010a), and Kuhnert et al. (2014b) found that some metabolites are apparently species-specific. This fact can substantially facilitate linking freshly collected specimens to old herbarium material of which molecular and sometimes even morphological data are lacking.

For taxonomic purposes, in fresh specimens, morphological data may be combined with chemical techniques

E. B. Sir
Consejo Nacional de Investigaciones Científicas y Técnicas (CONICET), Av. 13 Rivadavia 1917, Buenos Aires C1033AAJ, Argentina

E. B. Sir
Fundación Miguel Lillo, Laboratory Mycology, Miguel Lillo 251, San Miguel de Tucumán CP 4000, Tucumán, Argentina

E. Kuhnert · F. Surup · M. Stadler
Department of Microbial Drugs, Helmholtz-Zentrum für Infektionsforschung GmbH, Inhoffenstrasse 7, 38124 Braunschweig, Germany

E. Kuhnert · F. Surup · M. Stadler (✉)
German Centre for Infection Research (DZIF), Partner Site Hannover-Braunschweig, 38124 Braunschweig, Germany
e-mail: Marc.Stadler@t-online.de

K. D. Hyde
Institute of Excellence in Fungal Research and School of Science, Mae Fah Luang University, Chiang Rai 57100, Thailand

and molecular PCR-based methods. Molecular phylogenetic data are recognized as reliable support, in some cases, to resolve relationships within the subfamily Hypoxyloideae. Different authors revealed the applicability of several DNA loci like ITS rDNA, β -tubulin, and α -actin, which are suitable to distinguish species or to evaluate phylogenetic relationships (Kuhnert et al. 2014a). Hsieh et al. (2005) segregated the species formerly included in *Hypoxylon* sect. *Annulata* s. Ju and Rogers (1996) and erected the genus *Annulohypoxylon* based on micro-morphological characteristics, corroborated by molecular phylogenetic data.

During our short-term surveys of members of the Hypoxyloideae in Thailand, we found more than 40 different species. Among these collections, approximately 30 % represented new taxa. Several recent studies had already revealed the extraordinary diversity of the Thai Xylariaceae (Suwannasai et al. 2005; Fournier et al. 2010a, b; Læssøe et al. 2010, 2013). We are particularly interested in one of our recent *Hypoxylon* collections from this country because of the occurrence of dimorphic stromatal surface colours on the same trunk. In addition, the material yielded large amounts of stromata for the chemical investigations.

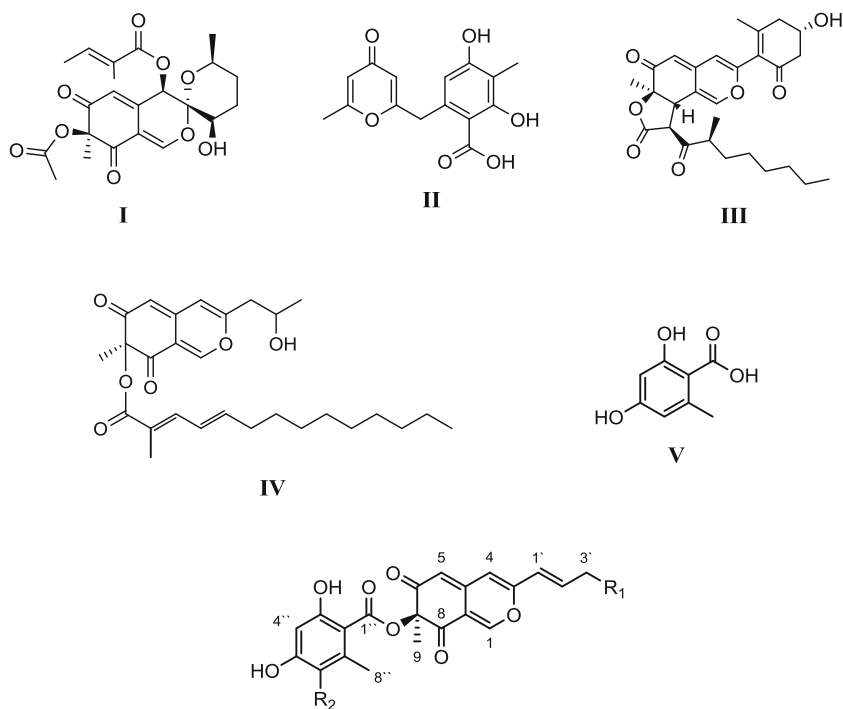
The current paper is, therefore, dedicated to the description of this *Hypoxylon* species from Thailand and the characterization of two novel, apparently specific azaphilones from its stromata.

Materials and methods

General

If not indicated otherwise, solvents were obtained in analytical grade from J.T. Baker (Deventer, Netherlands) or Merck (Darmstadt, Germany). Bold Arabic and Roman numbering refers to the chemical structures depicted in Fig. 1. All scientific names of fungi follow the entries in Mycobank (www.mycobank.org), hence no authors and years of publication are given. Reference specimens, including the designated type material of the new species, are housed in MFLU (Mae Fah Luang University, Chiang Rai, Thailand), and corresponding reference cultures have been deposited with MFLUCC (Chiang Rai, Thailand). Herbaria and culture collection acronyms are from Index Herbariorum (<http://sciweb.nybg.org/science2/IndexHerbariorum.asp>).

Fig. 1 Chemical structures of various stromatal metabolites isolated from *Hypoxylon fulvosulphureum* (1–4) or produced by other members of the Xylariaceae (I–VI). **I**, Daldinin C; **II**, macrocarpone A; **III**, cohaerin C; **IV**, rubiginosin C; **V**, orsellinic acid; **VI**, (+)-mitorubrin; **1**, (+)-6''-hydroxymitorubrinol acetate; **2**, (+)-mitorubrinol acetate; **3**, (+)-6''-hydroxymitorubrinol; **4**, (+)-mitorubrinol



VI: $R_1 = H, R_2 = H$

1: $R_1 = OAc, R_2 = OH$

2: $R_1 = OAc, R_2 = H$

3: $R_1 = OH, R_2 = OH$

4: $R_1 = OH, R_2 = H$

Morphological characterization

Teleomorphic structures were measured from fresh material mounted in distilled water, 5 % KOH and 10 % KOH. Melzer's reagent was used to test for the amyloid reaction (without KOH pretreatment). Anamorphic structures were observed microscopically in water or 5 % KOH. The number of the perithecia, asci, apical apparatus, ascospores, conidiogenous cells, and conidia that were used to calculate average size in the descriptions are 10, 20, 20, 40, 10, and 20, respectively. The descriptions of the teleomorph and branching pattern of conidiogenous structures follow Ju and Rogers (1996). The colour codes of the stromata and the extractable pigments follow Rayner (1970). Photos of micro-morphological structures were taken through a brightfield microscope at 400–1000 \times magnification. The cultures of the specimen were obtained from multispore isolates, using yeast-malt-glucose-agar (YMG: yeast extracts 4 g/l; malt extract 10 g/l; dextrose 4 g/l; cf. Bitzer et al. 2008) and Difco Oatmeal Agar (OA).

HPLC profiling

For HPLC analyses, stromata were extracted with methanol (Stadler et al. 2001b). Samples were analyzed by analytical HPLC (Agilent 1260 Infinity Series) equipped with a diode array detector and an ESI-iontrap MS detector (Amazon, Bruker). The instrumental settings were the same as described by Kuhnert et al. (2014b). Spectra were compared to an internal database with stored signals from standards of known secondary metabolites produced by Xylariaceae from previous work (Bitzer et al. 2007).

Molecular phylogenetic analyses

DNA isolation and sequence generation of the ITS region of the ribosomal RNA (spanning ITS1, 5.8S rDNA, ITS2 as well as partial 18S and 28S rDNA) as well as the β -tubulin coding gene (TUB) was carried out as described by Kuhnert et al. (2014b). In total, seven ITS and six β -tubulin sequences of various Asian Xylariaceae strains (including the newly described species) were obtained. Origin and culture collection numbers of the Asian material are summarized in Table 1. Each set of sequences was aligned with a selection of Xylariaceae sequences originating from previously published studies (for details, see Table 1). The backbone tree was composed of 30 representatives of the genus *Hypoxylon*, seven *Annulohypoxylon* spp., four *Daldinia* spp., and one *Astrocystis* species. The phylogenetic analyses were performed for each gene by using maximum likelihood (ML) as optimality criterion (Kuhnert et al. 2014a). Phylogenetic reconstruction of the ML tree was estimated with the software RAxML (Stamatakis 2006) applying the GTRCAT rate

distribution model (with 25 rate categories) and the rapid bootstrap analysis algorithm. The program executed 1,000 bootstrap (BS) replicates, the support values of which were mapped onto the most likely tree topology found by an independently executed search. Branch lengths were thereby calculated based on base exchange rates. The following deviations from the protocol (Kuhnert et al. 2014a) were applied due to alignability issues: 331 reliably alignable base pair positions 25–44, 46–61, 280–291, 320–328, 339–543, 552–584, and 586–616 according to the sequence JX183075 (*H. pulicidum*) were included in the ITS analysis and 1,031 base pair positions 137–149, 159–195, 239–356, 260–345, 385–456, 503–509, and 523–1320 of JX183072 (*H. pulicidum*) were considered in the β -tubulin analysis. Both trees were rooted with *Astrocystis bambusae* (KP401580 and KP401587, respectively).

Extraction and isolation of stromatal pigments

Stromata of the collection EK13010 (total weight of 1 g) were detached from their woody substratum and extracted with 100 ml acetone for 30 min in an ultrasonic bath. The organic phase was separated from the stromata and the previous step was repeated twice. The solvent extracts were combined and evaporated to yield 400 mg of crude extract. The crude material was dissolved in acetonitrile and filtered through an RP solid phase cartridge (Strata-X 33 mm, Polymeric Reversed Phase; Phenomenex Aschaffenburg, Germany) and separated by preparative HPLC (PLC 2020, Gilson, Middleton, WI, USA). A VP Nucleodur C18 ec column (125 \times 40 mm, 7 μ m; Macherey-Nagel) was used as stationary phase. The mobile phase was composed of deionized water (solvent A, Milli-Q, Millipore, Schwalbach, Germany) and acetonitrile (solvent B). The gradient was set from 20 to 100 % solvent B in 40 min followed by 15 min isocratic conditions applying a flow rate of 30 ml/min. UV detection was carried out at 210 nm and 254 nm and fractions were collected and combined according to the observed peaks. The separation yielded four compounds in pure amounts with the main compound **1** (37 mg) at a retention time (Rt)=19–21 min, **2** (13 mg) at Rt=23 min, **3** (4 mg) at Rt=14–15 min, and **4** (3 mg) at Rt=17 min.

(+)-6''-Hydroxymitorubrinol acetate (**1**): Yellow oil, $[\alpha]_D^{25} +419$ (c 0.1, dioxan); UV (CH₃CN) λ_{max} (log ϵ) 237 nm (4.30), 263 nm (4.35), 342 nm (4.38); ¹H NMR (700 MHz, CDCl₃) see Table 3, ¹³C NMR (175 MHz, CDCl₃) see Table 2; ESIMS m/z 457.0 [M+H]⁺, 455.1 [M-H]⁻; HRESIMS m/z 457.1128 [M+H]⁺ (calcd for C₂₃H₂₁O₁₀, 457.1129).

(+)-Mitorubrinol acetate (**2**): Yellow oil; ¹H NMR (700 MHz, CDCl₃) see Table 3, ¹³C NMR (175 MHz, CDCl₃) see Table 2; ESIMS m/z 441.0 [M+H]⁺, 439.0 [M-H]⁻; HRESIMS m/z 441.1182 [M+H]⁺ (calcd for C₂₃H₂₁O₉, 441.1180).

Table 1 List of used taxa for phylogenetic reconstruction

Species	GenBank Acc. No. β -tubulin	GenBank Acc. No. ITS	Specimen or strain ID	Origin	Reference
<i>Annulohyphoxylon annulatum</i>	KC977276	AM749938	MUCL 47218	China	Bitzer et al. (2008), Kuhnert et al. (2014a)
<i>A. atrorseum</i>	KP401588	KP401581	MFLUCC 14-1220	Thailand	This study
<i>A. bovei</i> var. <i>microspora</i>	AY951654	EF026141	BCRC 34012	Taiwan	Hsieh et al. (2005)
<i>A. minutellum</i>	AY951659	–	BCRC34017	Taiwan	Hsieh et al. (2005)
	–	JX658447	CBS 119015	Portugal	Stadler et al. (2014)
<i>A. nitens</i>	KC977275	KC968927	CBS 119134	Guadeloupe	Kuhnert et al. (2014a)
<i>A. stygium</i>	KP401586	KP401579	BCC 71968	Thailand	This study
<i>A. urceolatum</i>	KP401585	KP401578	MFLUCC 14-1228	Thailand	This study
<i>Astrocystis bambusae</i>	KP401587	KP401580	MFLUCC 14-1219	Thailand	This study
<i>Daldinia childiae</i>	AY951691	–	BCRC 34044	Hawaii (USA)	Hsieh et al. (2005)
	–	JX658462	MUCL 46818	France	Stadler et al. (2014)
<i>D. concentrica</i>	KC977274	AY616683	CBS 113277	Germany	Triebel et al. (2005), Kuhnert et al. (2014a)
<i>D. eschscholtzii</i>	KC977266	JX658484	MUCL 45435	Benin	Stadler et al. (2014), Kuhnert et al. (2014a)
<i>D. placentiformis</i>	KC977278	AM749921	MUCL 47603	Mexico	Bitzer et al. (2008), Kuhnert et al. (2014a)
<i>Hypoxylon cinnabarinum</i>	AY951709	JN979409	BCRC33810	Mexico	Hsieh et al. (2005)
<i>H. crocopeplum</i>	KC977268	KC968907	CBS 119004	France	Kuhnert et al. (2014a)
<i>H. erythrostroma</i>	KC977296	KC968910	MUCL 53759	Martinique	Kuhnert et al. (2014a)
<i>H. fendleri</i>	AY951718	JN979418	BCRC 34064	Taiwan	Hsieh et al. (2005)
<i>H. fragiforme</i>	AY951719	–	BCRC 34065	France	Hsieh et al. (2005)
	–	AY616690	CBS 114745	Germany	Triebel et al. (2005)
<i>H. fulvo-sulphureum</i>	KP401584	KP401576	MFLUCC 13-0589	Thailand (T)	This study
	–	KP401577	MFLUCC 13-0590	Thailand	This study
<i>H. fuscum</i>	AY951723	JN979423	BCRC 34069	Taiwan	Hsieh et al. (2005)
<i>H. griseobrunneum</i>	KC977281	KC968928	MUCL 53310, CBS 129346	Guadeloupe	Kuhnert et al. (2014a)
<i>H. haematostroma</i>	KC977291	KC968911	MUCL 53301	Martinique (ET)	Kuhnert et al. (2014a)
<i>H. hypomiltum</i>	KC977298	KC968914	MUCL 53312, CBS 129036	Guadeloupe	Kuhnert et al. (2014a)
<i>H. investiens</i>	KC977270	KC968925	CBS 118183	Malaysia	Bitzer et al. (2008), Kuhnert et al. (2014a)
<i>H. isabellinum</i>	KC977295	KC968935	MUCL 53308, CBS 129035	Martinique (T)	Kuhnert et al. (2014a)
<i>H. jaklitschii</i>	KM610304	KM610290	CBS 138916	Sri Lanka (T)	Kuhnert et al. (2015)
<i>H. jecorinum</i>	AY951731	JN979429	N/A	Mexico	Hsieh et al. (2005)
<i>H. laminosum</i>	KC977292	KC968934	MUCL 53305, CBS 129032	Martinique (T)	Kuhnert et al. (2014a)
<i>H. lateripigmentum</i>	KC977290	KC968933	MUCL 53304, CBS 129031	Martinique (T)	Kuhnert et al. (2014a)
<i>H. lenormandii</i>	KM610305	KM610289	MFLUCC 13-0580, BCC 71961	Thailand	Kuhnert et al. (2015)
<i>H. lividicolour</i>	AY951734	JN979432	BCRC 34076	Taiwan (T)	Hsieh et al. (2005)
<i>H. monticulosum</i>	KP401578	KP401585	MFLUCC 13-0593, BCC 71965	Thailand	This study
<i>H. nicaraguense</i>	KC977272	AM749922	CBS 117739	Burkina Faso	Bitzer et al. (2008)
<i>H. ochraceum</i>	KC977300	KC968937	MUCL 54625	Martinique (ET)	Kuhnert et al. (2014a)
<i>H. perforatum</i>	KC977299	KC968936	MUCL 54174	Japan	Kuhnert et al. (2014a)
<i>H. pilgerianum</i>	AY951744	JQ009310	BCRC 34985	Taiwan	Hsieh et al. (2005)
<i>H. polyporoideum</i>	AY951747	JQ009311	BCRC 34088	Taiwan	Hsieh et al. (2005)
<i>H. pulicidum</i>	JX183072	JX183075	MUCL 49879, CBS 122622	Martinique (T)	Bills et al. (2012)

Table 1 (continued)

Species	GenBank Acc. No. β -tubulin	GenBank Acc. No. ITS	Specimen or strain ID	Origin	Reference
<i>H. rickii</i>	KC977288	KC968932	MUCL 53309, CBS 129345	Martinique (ET)	Kuhnert et al. (2014a)
<i>H. samuelsii</i>	KC977286	KC968916	MUCL 51843	Guadeloupe (ET)	Kuhnert et al. (2014a)
<i>H. sublenormandii</i>	KM610303	KM610291	CBS 138917	Sri Lanka	Kuhnert et al. (2015)
<i>H. tortisporum</i>	KF300546	KF234420	BCC 62413	Thailand	Kuhnert et al. (2014a)
<i>H. trugodes</i>	KF300548	KF234422	MUCL 54794	Sri Lanka (ET)	Kuhnert et al. (2014a)

GenBank accession numbers, Specimen ID of public culture collections or herbaria (if available), origin, and reference studies are given. Type specimens are labelled with **T** (holotype) or **ET** (epitype).

Spectroscopic and spectrometric data were in good agreement with the literature (Steglich et al. 1974; Stadler et al. 2001).

(+)-6''-Hydroxymitorubrinol (**3**): Yellow oil, $[\alpha]_D^{25} +378$ (c 0.1, dioxan); UV (CH₃CN) λ_{max} (log ϵ) 238 nm (4.07), 263 nm (4.15), 344 nm (4.18)); ¹H NMR (700 MHz, CDCl₃) see Table 3, ¹³C NMR (175 MHz, CDCl₃) see Table 2; ESIMS m/z 415.0 [M+H]⁺, 413.0 [M-H]⁻; HRESIMS m/z 415.1022 [M+H]⁺ (calcd for C₂₁H₁₉O₉, 415.1024).

(+)-Mitorubrinol (**4**): Yellow oil; ¹H NMR (700 MHz, CDCl₃) see Table 3, ¹³C NMR (175 MHz, CDCl₃) see Table 2; ESIMS m/z 399.0 [M+H]⁺, 397.0 [M-H]⁻; HRESIMS m/z 399.1076 [M+H]⁺ (calcd for C₂₁H₁₉O₈, 399.1074).

Table 2 ¹³C NMR data of pigments **1–4** in acetone-*d*₆ (175 MHz)

	(1)	(2)	(3)	(4)
1	155.6, CH	155.0, CH	155.2, CH	155.0, CH
3	156.1, C	155.5, C	156.6, C	156.5, C
4	112.1, CH	111.5, CH	110.3, CH	110.2, CH
4a	144.1, C	143.5, C	144.1, C	144.1, C
5	109.2, CH	108.6, CH	108.1, CH	108.0, CH
6	192.9, C	192.1, C	192.4, C	192.0, C
7	87.1, C	86.6, C	86.6, C	86.6, C
8	193.6, C	192.9, C	193.2, C	193.0, C
8a	116.3, C	115.7, C	115.8, C	115.7, C
9	23.2, CH ₃	22.6, CH ₃	22.8, CH ₃	22.7, CH ₃
1'	123.8, CH	123.2, CH	120.1, CH	120.0, CH
2'	133.8, CH	133.2, CH	140.3, CH	140.2, CH
3'	64.3, CH ₂	63.7, CH ₂	62.1, CH ₂	62.0, CH ₂
1''	171.1, C	170.5, C	170.6, C	170.5, C
2''	105.5, C	105.0, C	105.1, C	105.1, C
3''	158.9, C	166.1, C	158.5, C	166.0, C
4''	101.9, CH	101.6, CH	101.4, CH	101.6, CH
5''	153.4, C	163.8, C	152.9, C	163.8, C
6''	138.3, C	112.5, CH	137.9, C	112.5, CH
7''	127.8, C	144.8, C	127.3, C	144.7, C
8''	15.3, CH ₃	23.9, CH ₃	14.8, CH ₃	23.9, CH ₃
1'''	171.1, C	170.5, C		
2'''	21.3, CH ₃	20.6, CH ₃		

Spectroscopic and spectrometric data were in good agreement with the literature (Steglich et al. 1974; Stadler et al. 2001).

Structure elucidation

Optical rotations were determined with a PerkinElmer 241 polarimeter and UV–vis spectra were recorded with a Shimadzu (Kyoto, Japan) UV–vis spectrophotometer UV-2450. NMR spectra were recorded with a Bruker (Bremen, Germany) Avance III 700 spectrometer with a 5 mm TXI cryoprobe (¹H 700 MHz, ¹³C 175 MHz) or a Bruker Avance III 500 (¹H 500 MHz). Electrospray ionization mass spectrometry (ESIMS) spectra were obtained with an ion trap mass spectrometer (MS, Amazon, Bruker) and HRESIMS spectra with a time-of-flight MS (Maxis, Bruker) as described by Pažoutová et al. (2013).

Bioactivity assay

Minimum inhibitory concentrations (MIC) were estimated with a serial dilution assay with pure substances dissolved in acetonitrile using various test organisms for antibacterial and antifungal activity (Halecker et al. 2014). The in vitro cytotoxicity assay with the mouse fibroblast cell line L929 was performed as previously reported (Okanya et al. 2011). As a minor change, the solvent (methanol) was replaced by acetonitrile.

Results

The unique combination of morphological, molecular, and chemotaxonomic data led to the conclusion that *Hypoxylon fulvo-sulphureum* represented an undescribed species of the Xylariaceae, and therefore, is described as new.

Taxonomic part

Hypoxylon fulvo-sulphureum Kuhnert & Sir, sp. nov. Fig. 2
Mycobank MB811162

Table 3 ^1H NMR data of pigments **1**–**4** in acetone- d_6 (700 MHz)

	(1)	(2)	(3)	(4)
1	8.14, m	8.13, m	8.14, m	8.13, m
4	6.65, s	6.65, brs	6.60, s	6.60, brs
5	5.65, d (1.2)	5.64, d (1.2)	5.63, d (1.2)	5.62, d (1.2)
9	1.66, s	1.66, s	1.65, s	1.66, s
1'	6.50, dt (15.8, 1.7)	6.49, dt (15.8, 1.7)	6.47, dt (15.6, 2.0)	6.47, dt (15.6, 2.1)
2'	6.62, m	6.62, dt (15.8, 5.2)	6.73, dt (15.6, 4.1)	6.73, dt (15.6, 4.1)
3'	4.80, dd (5.2, 1.7)	4.79, dd (5.2, 1.7)	4.34, dd (4.1, 2.0)	4.34, brs
4''	6.30, s	6.23, d (2.6)	6.30, s	6.23, d (2.6)
6''		6.36, brd (2.6)		6.35, dq (2.6, 0.8)
8''	2.55, s	2.60, s	2.55, s	2.60, brs
3''-OH	10.14, s	10.74, s	10.14, s	10.75, s
2'''	2.09, s	2.09, s		

Etymology: In reference to its orange-brown and sulphur-yellow stromatal surface colours.

Known distribution: Thailand

Holotype: **Thailand**, Chiang Rai Province, on wood, 16 Aug. 2013, leg. Benjarong Thongbai and Eric Kuhnert, EK 13010 (MFLU 13–0352, ex-type culture MFLUCC 13–0589; GenBank Acc. No: ITS – KP401576, β -tubulin – KP401584).

Additional specimen; Chiang Rai Province, on wood, 16 Aug. 2013, leg. Benjarong Thongbai and Eric Kuhnert, EK 13011 (MFLU 13–0353, culture MFLUCC 13–0590; GenBank Acc. No: ITS – KP401577).

A totis speciebus Hypoxylon differt stromatibus maturis conspicuis bicoloribus, superficie fusca vel sulphurea. A Hypoxylon cinnabarinum et H. crocopleum differt stromatibus altiores, peritheciae maiora, usque at in ascosporae (12–)13–15(–16) × 5–6(–6.5) μm perisporium, conspicuiter striatum, praeditae. A Hypoxylon jecorinum differt ascosporae parviorae usque at statu anamorphosis ad genero Periconiella similis. A Hypoxylon erythrostoma differt ascosporae parviorae usque at granulis aurantiacis, peritheciis ambientibus.

Stromata effused-pulvinate; 5–43 mm long × 2–12 mm broad × 0.6–1 mm thick; with inconspicuous perithecial mounds; Fulvous (43) or Sulphur Yellow (15); pruinose; orange to red granules immediately beneath the surface and between perithecia; with KOH extractable pigment Orange (7) to Red (2); tissue below the perithecial layer inconspicuous, brown to black, 0.1–0.3 mm thick. *Perithecia* ovoid or ob-ovoid, laterally compressed, 0.3–0.5 mm high × 0.2–0.3 mm diam, ostiolar openings lower than the stromatal surface, umbilicate with white area surrounding ostioles in the fulvous stromata. *Asci* 8-spored, eventually 6-spored, cylindrical, 125–210 μm total length, the spore-bearing parts 75–90 μm × 6.5–9 μm wide, stipes 32–120 μm long, with amyloid, the discoid apical apparatus 1–1.5 μm high × 2–3 μm broad. *Ascospores* brown, ellipsoid-inequilateral, with narrowly rounded ends, slightly curved, (12–)13–15(–16) × 5–6(–6.5)

μm, with straight to slightly sigmoid germ slit spore-length at convex side; perispore dehiscent in KOH, with conspicuous coil-like ornamentation; epispore smooth.

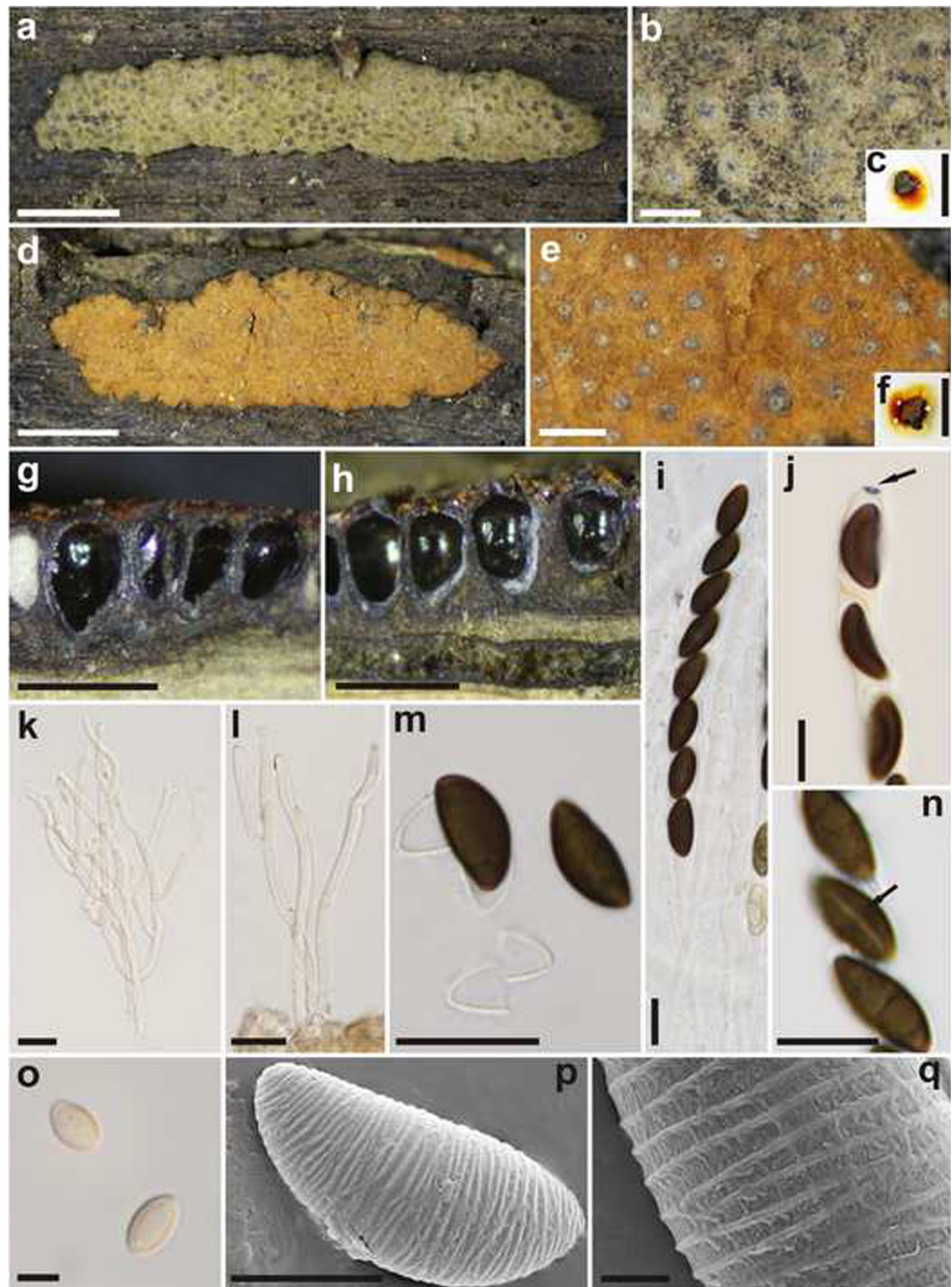
Asexual morph on natural substratum: *Conidiogenous structure* on young stromata virgariella-like. *Conidiophores* pale brown to hyaline, finely roughened. *Conidiogenous cells* pale yellow to hyaline, smooth, 5–72 × 2–3.5 μm. *Conidia* ellipsoid, pale brown to hyaline, smooth, 5–8 × 3–4(–5) μm.

Culture Colonies on YM 6.3 covering a 90 mm Petri dish in a week, at first whitish, becoming Sulphur Yellow (15) or Pale Luteous (11), velvety to felty, mildly zonate, with entire margin; reverse Honey (64). Not sporulating. Colonies on OA (90 mm Petri dish) slow growing, reaching a diameter of 5.0 cm in 30 days, floccose, azonate, with entire margins, mycelium whitish; reverse colorless. No conidiogenous structures were observed.

Secondary metabolites The stromatal HPLC/DAD/MS profile is characterized by (+)-6''-hydroxymitorubrinol acetate (**1**) as a major metabolite as well as (+)-mitorubrinol acetate (**2**), (+)-6''-hydroxymitorubrinol (**3**), and (+)-mitorubrinol (**4**) as minor constituents. Furthermore, another yet unidentified azaphilone with $M=474$ Da (m/z 475.2327 $[M+H]^+$; calcd for $C_{26}H_{35}O_8$, 475.2326) was detected. Mitorubrin and orsellinic acid, however, could only be detected in traces. The relative amounts of **3** and **4** were apparently lower in the sulphur-coloured stromata (Fig. 3).

Notes Notably, *Hypoxylon fulvo-sulphureum* is characterized by having mature stromata occurring together on the same substratum with two different stomatal surface colours. Mixed bicoloured stromata, to our knowledge, have never been reported for other species of *Hypoxylon*. Normally, variable colours are attributed to a succession of immature, mature to weathered stromata of a given species. However, our morphological, chemotaxonomic, and molecular phylogenetic

Fig. 2 *Hypoxylon fulvo-sulphureum*. **a**: stromatal habit, **b**: close-up view of stromatal surface, **c**: pigment in KOH. **d**: stromatal habit stomata, **e**: close-up view of stromatal surface, **f**: pigment in KOH. **g, h**: section through stroma showing perithecia. **i**: asci. **j**: apical ring in Melzer's reagent. **k, l**: conidiogenous structure. **m**: ascospores in KOH whit dehiscent perispore. **n**: ascospores showing germ slit (*arrow*). **o**: conidia. **p, q**: SEM microphotographs of the conspicuously ornamented perispore. **a–c, g, i–q**: specimen EK13010. **d–f, h**: specimen EK13011. Scale bars: a, c, d, f: 3 mm. b, e, g, h: 0.5 mm. i, j, k, l, n: 10 μ m. o, p: 5 μ m. q: 1 μ m, m: 15 μ m

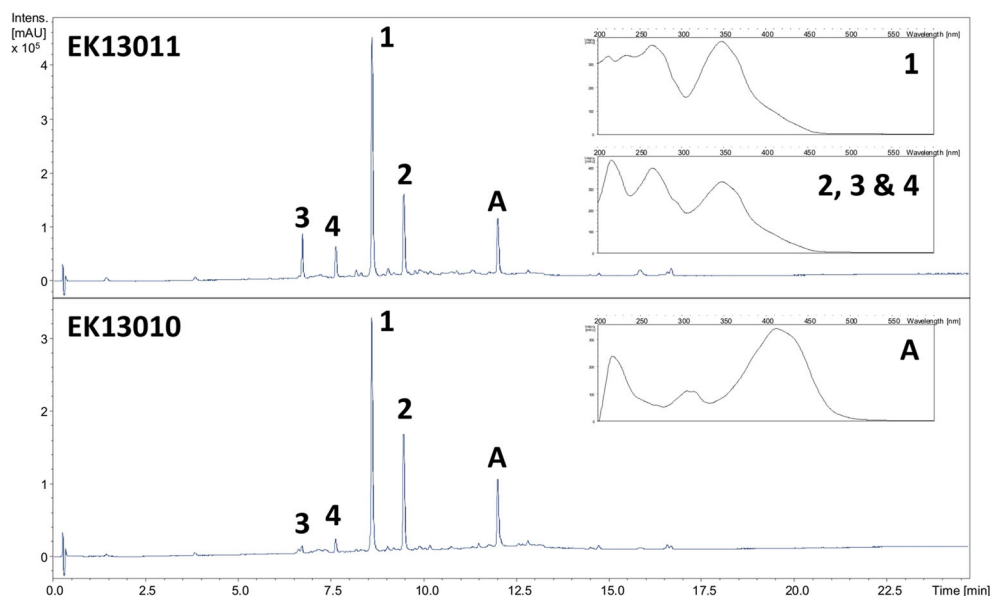


analyses unequivocally showed that both phenotypes represented the same species.

The sulphur-yellow stromata of the new taxon are striking; young stromata of other species of *Hypoxylon* may also occasionally attain similar colours, but only if the stromata have not yet produced asci. The fulvous stromata of *H. fulvo-sulphureum* may be confused with *H. cinnabarinum*, *H. crocopeplum*, and *H. jecorinum*, but they differ in having thicker stromata and tubular perithecia. In addition, *H. cinnabarinum* has nearly equilateral ascospores, a germ slit less spore-length and a smooth perispore, whereas

H. crocopeplum has larger ascospores ($9\text{--}17.5 \times 4\text{--}7.5 \mu\text{m}$ vs. $12\text{--}16 \times 5\text{--}6.5 \mu\text{m}$) and larger perithecia ($0.2\text{--}1.5 \times 0.1\text{--}0.4 \text{ mm}$ vs. $0.3\text{--}0.5 \times 0.2\text{--}0.3 \text{ mm}$). In contrast, *H. jecorinum* differs in having smaller ascospores ($8\text{--}11 \times 4\text{--}5 \mu\text{m}$ vs. $12\text{--}16 \times 5\text{--}6.5 \mu\text{m}$) and in having a periconiella-like conidiogenous structure. The stromatal pigments of all four species are mitorubrin derivatives. However, only *H. fulvo-sulphureum* contains (+)-6"-hydroxymitorubrinol acetate (**1**) and (+)-6"-hydroxymitorubrinol (**3**). Moreover, *Hypoxylon crocopeplum* contains rubiginosins in addition to the "regular" mitorubrins (cf. Quang et al. 2006; Stadler et al. 2008).

Fig. 3 Stromatal HPLC-UV profiles derived from EK13010 and EK13011 and the DAD spectra of (+)-6"-hydroxymitorubrinol acetate (**1**), (+)-mitorubrinol acetate (**2**), (+)-6"-hydroxymitorubrinol (**3**), (+)-mitorubrinol (**4**) and an unidentified azaphilone (**A**)

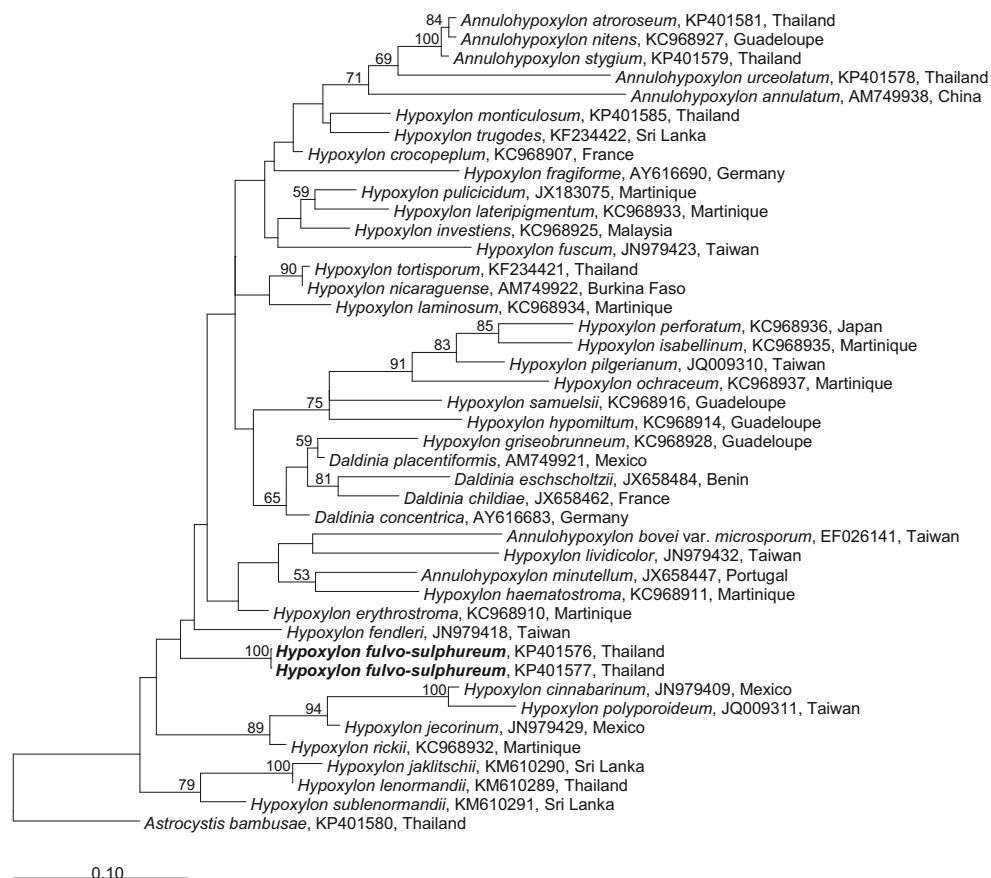


Molecular phylogeny

In total, 43 sequences of the ITS region and 42 sequences of the partial β -tubulin gene (TUB) were selected for the phylogenetic study (Figs. 4 and 5). The selection focused on sequences derived from Asian material to give a more

reasonable assessment of the phylogenetic position concerning the new species. Twenty-one sequences of each gene were obtained from *Hypoxylon* species and closely related allies of Asian origin. To fill out the tree, selected tropical species of the Hypoxyloideae and the type species of *Hypoxylon* (*H. fragiforme*) as well as *Daldinia*

Fig. 4 Phylogenetic relationships among *Hypoxylon fulvo-sulphureum* (highlighted in bold) and related Xylariaceae as inferred from internal transcribed spacer (ITS) rRNA gene sequences. Maximum Likelihood (ML) bootstrap support values above 50 %, from 1,000 RAxML replicates are assigned to the tree topology of the most likely tree found by RAxML. Species names are followed by the Genbank accession number and countries of origin



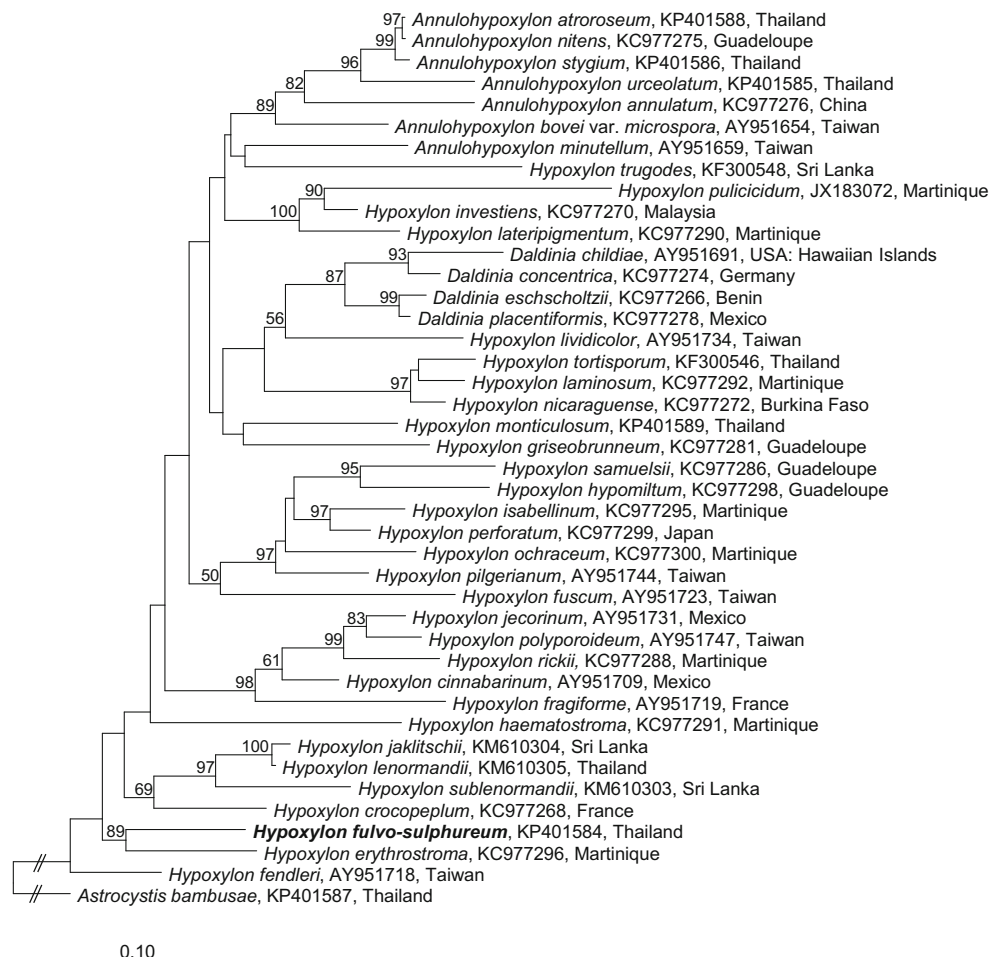
(*D. concentrica*) were included. Furthermore, sequences of European *A. minutellum*, *D. childiae*, and *H. crocopeplum* were included. The latter was chosen to evaluate the comparability between morphological and phylogenetic relationships of *H. fulvo-sulphureum*. Both trees showed a weakly supported backbone. In the ITS reconstruction, all genera appeared polyphyletic, whereas in the TUB analyses *Daldinia* was monophyletic. In some preliminary TUB calculations, the genus *Annulohypoxylon* had appeared monophyletic (data not shown), because the position of *H. trugodes* can vary within the tree. The ITS sequences derived from cultures of the differently coloured *H. fulvo-sulphureum* stromata were identical and provided additional proof that the morphologically deviating stromata of the type specimen actually belonged to the same species. In addition, the sequences formed an unsupported clade with *H. fendleri*. The latter can be easily distinguished from the new species by much darker surface colours, smaller ascospores, and inconspicuous perispore ornamentation. No close phylogenetic relationship to *H. cinnabarinum*, *H. crocopeplum*, or *H. jecorinum* was evident. In the TUB tree, *H. fulvo-sulphureum* formed a well-supported (89 %) branch with *H. erythrostroma*, but as inferred from this

phylogenetic tree, the new species had no apparent close phylogenetic relationship to morphologically similar species. *Hypoxylon erythrostroma* has less in common with *H. fulvo-sulphureum* except the production of mitorubrin-type azaphilones.

Structure elucidation

Four yellow pigments were obtained by preparative HPLC. The HRESIMS data of major compound **1** supported a molecular formula of $C_{23}H_{20}O_{10}$, implying 14 degrees of unsaturation. The UV spectrum showed an absorbance maxima at 237, 263, 342 nm, which is characteristic of an azaphilone moiety, a common scaffold (Gao et al. 2013) for pigments of *Hypoxylon* species. Proton (Table 3) and $^1H,^{13}C$ HSQC spectra exhibited signals for three singlet methyls, six olefinic protons, one oxygenated methylene, and one exchangeable proton presumably bound to an oxygen. The carbon NMR (Table 2) spectrum revealed the further presence of four carbonyls, four oxygenated, and four non-oxygenated quaternary sp^2 carbons and one oxygenated sp^3 hybridized one.

Fig. 5 Phylogenetic relationships among *Hypoxylon fulvo-sulphureum* (highlighted in bold) and related Xylariaceae as inferred from β -tubulin gene sequences. Maximum Likelihood (ML) bootstrap support values above 50 %, from 1,000 RAxML replicates are assigned to the tree topology of the most likely tree found by RAxML. Species names are followed by the GenBank accession number and countries of origin



Correlations from 1' to 3' in the ^1H , ^1H COSY NMR spectrum established the 3-hydroxypropenyl side chain. ^1H , ^{13}C HMBC correlations from H-1 to C-3, C-4a, C-8; from H-4 to C-3, C-5, C-8a, C-1'; from H-5 to C-4, C-7, C-8a, from H₃-9 to C-6, C-7, C-8, and from H-1' to C-4 identified the carbon backbone of the core metabolite. The deep field shift of H₂-3' indicated an ester bonding at this position, which was confirmed by ^1H , ^{13}C HMBC correlations from H₂-3' and H₃-2''' to C-1''' and established the mitorubrinol acetate (**2**)-type partial structure. However, in comparison to **2** the orsellinic acid moiety was significantly changed with the absence of a proton signal for H-6'' and relative upfield shifts of C-3'', C-5'', C-7''. The hydroxylation of the orsellinic acid unit at 6'' position was deduced from of ^1H , ^{13}C HMBC correlations from H₃-8'' to C-2'', C-6'', C-7'', and H-4'' to C-2'', C-6'', C-3'', C-5'', C-1'' (the latter three were weaker 2J and 4J correlations). The stereochemistry at C-7 in **1** was determined to be *S* from the optical rotation ($[\alpha]_{\text{D}} +419$) (Suzuki et al. 1999). Thus, the structure of pigment **1** was established as (+)-6''-hydroxymitorubrinol acetate.

The molecular formula of **2**, which was deduced from its $[\text{M}+\text{H}]^+$ peak in the HRESIMS spectrum, indicated the presence of one oxygen atom less in comparison to **1**. The proton NMR spectrum of **2** showed one additional aromatic methine signal, which was identified as H-6'' of orsellinic acid by ^1H , ^{13}C HMBC correlations. Therefore, compound **2** was identified as the known (+)-mitorubrinol acetate.

Metabolite **3** showed a molecular ion cluster at m/z 415.1022, comprising a molecular formula of $\text{C}_{21}\text{H}_{19}\text{O}_9$ and in consequence indicating the loss of $\text{C}_2\text{H}_2\text{O}$ compared to **1**. Proton and carbon NMR spectra of **3** were basically identical to **1** with the exception of the shortfall of the signals for the acetyl moiety and the upfield shift of H₂-3' (4.34 ppm in **3**; 4.80 ppm in **1**). The stereochemistry at C-7 in **1** was determined to be *S* from the optical rotation ($[\alpha]_{\text{D}} +378$) (Suzuki et al. 1999). Consequently, compound **3** was established as the new natural product (+)-6''-hydroxymitorubrinol (**3**).

The molecular formula $\text{C}_{21}\text{H}_{18}\text{O}_8$ of pigment **4** was concluded on the basis of its HRESIMS cluster at m/z 399.1074. Compared to **2**, signals of the acetyl group were missing in the proton and carbon NMR spectra along an upfield shift of H₂-3'. Thus, **4** was identified as (+)-mitorubrinol.

Bioactivity of **1** – **4**

Compounds **1** – **4** were inactive in the antifungal and antibacterial assays. The metabolites **1** and **2** exhibited IC_{50} values of 21 $\mu\text{g}/\text{ml}$ in the cytotoxicity assay against the mouse fibroblast cell line L929, whereas **3** and **4** were inactive.

Discussion

The azaphilones of the mitorubrin type are widely distributed within the genus *Hypoxylon*. These polyketide metabolites can be found in members of the temperate (e.g., *H. fragiforme*, *H. howeanum*) and tropical zones (e.g., *H. fendleri*, *H. haematostroma*, *H. rickii*) (Hellwig et al. 2005, Quang et al. 2006). The biosynthesis of these compounds within the Xylariaceae, and in the ascomycetes in general likely originated from common ancestral pathways rather than having developed independently multiple times during evolution. In the study of Kuhnert et al. (2014a), *Hypoxylon* species producing mitorubrin-type azaphilones were found to be closely related in the phylogenetic reconstructions. This supports the evolutionary hypothesis concerning the distribution of mitorubrin biosynthesis gene clusters. Curiously, previous studies on the genus *Entonaema* (Stadler et al. 2004, 2008) had revealed that several of its species, including the type species *E. liquescens*, also contain mitorubrins. Despite the fact that the occurrence of mitorubrin derivatives is common in *Hypoxylon*, the chemical patterns can strongly vary between the respective species. This is the first report of hydroxylated orsellinic acid moieties for the genus, but they are known from the azaphilones purpurquinone B (Wang et al. 2011) and 5''-hydroxy-2''-O-methylmitorubrin (Singh et al. 2006) produced by *Penicillium* spp. For some unknown reasons, sometimes a different mass (reduced by 2) occurred for the new compounds in methanolic crude extracts. The exact conditions leading to an oxidation of the two substances remains obscure. We studied the HPLC-DAD/MS profiles of various mitorubrin producers among the genus *Hypoxylon*. Compounds **1** and **3** were also detected in collections from Thailand with high similarity to *H. fendleri* (data not shown). However, thus far, the compounds are not known to occur in other geographical regions. Therefore, these metabolites are not reliable chemotaxonomic markers at the species level, but still can be valuable to discriminate closely related species. Interestingly, most of the analyzed species contained mitorubrinol (**4**) and mitorubrinol acetate (**2**) in their stromatal extracts; however, besides these compounds, they apparently produce different specific mitorubrin derivatives as minor components. For example, this is the case in *H. cinnabarinum* (M=400 Da) or *H. jecorinum* (M=412 Da).

The surface colour has been regarded as an important characteristic to discriminate species or to describe new taxa, even when it was known that the colour may vary during ontogeny. For example, melanisation is correlated with progressive darkening and eventual blackening of old stromata (Ju and Rogers 1996; see also Stadler et al. 2014 for the related *Daldinia*). However, when dealing with freshly collected, mature material, the diagnostic relevance of the surface colour has never been disputed. The case of *Hypoxylon fulvo-sulphureum* demonstrates the plasticity of this attribute even in mature collections. Both specimens were gathered from the same trunk,

where the two morphotypes grew intermingled. Some stromata even showed an intermediate pigmentation. Interestingly, the secondary metabolite profiles of the differently coloured stromata were identical, only varying in the relative concentration of the compounds. However, purified mitorubrin-type pigments in *Hypoxylon* are always yellow to orange, which cannot explain the yellow-greenish surface of some stromata. Further investigations are needed to clarify the causes for the dimorphic phenotypes. Another example where the surface colour has been shown to be of little diagnostic relevance in retrospective is the differentiation of *Annulohypoxylon atroroseum* and *A. stygium*. Originally, *A. atroroseum* (formerly *H. atroroseum*) was described due to its rose-coloured stromata (Rogers 1981). Meanwhile, it has been established that both species often share this character, and they can only be discriminated by their conidiogeneous structures (Ju and Rogers 1996). Therefore, description of new species of Xylariaceae solely on a morphological data (especially when the main diagnostic feature is the surface colour) should always be confirmed by chemotaxonomic and molecular phylogenetic data as corroborating evidence.

From a chemical point of view the exploration of *Hypoxylon* and closely related taxa in Thailand seems promising. Especially the members of *Annulohypoxylon* tend to produce numerous and large stromata which are often in sufficient quantities for preparative chemical studies. Abundant biomass facilitates the search for chemotaxonomic correlations and new bioactive natural products that eventually may be useful in pharmacological research.

Acknowledgments We gratefully acknowledge support from the curators of various international culture collections and herbaria, above all, BCC and MFLUCC, who provided important specimens for the present study.

The field sampling in Thailand benefited from a joint TRF-DAAD PPP academic exchange grant by the German Academic Exchange Service (DAAD) and the Thai Royal Golden Ph.D. Jubilee-Industry program (RGJ) to Kevin D. Hyde, Eric Kuhnert, and Marc Stadler. The DAAD and the Argentina Ministerio de Ciencia, Tecnología e Innovación Productiva are also gratefully acknowledged for an academic exchange grant involving Eric Kuhnert, Esteban Benjamin Sir and Marc Stadler.

We thank Simone Heitkämper for her excellent assistance in the molecular work and Benjarong Thongbai for help with the fieldwork. Furthermore, we are grateful to various colleagues at the HZI: Kathrin I. Mohr and Wera Collisi for conducting the bioassays and Christel Kakoschke for recording NMR spectra. Manfred Rohde is thanked for SEM recordings. For measurements of the HPLC–HRMS data we are grateful to Aileen Teichmann. We also thank Philine Wotsch for technical assistance in culture maintenance.

References

Bills GF, Gonzalez-Mendez V, Martin J, Platas G, Fournier J, Persöh D, Stadler M (2012) *Hypoxylon pulicidum* sp. nov. (Ascomycota, Xylariales), a pantropical insecticide-producing endophyte. PLoS ONE 7:e46687. doi:10.1371/journal.pone.0046687

- Bitzer J, Köpcke B, Stadler M, Hellwig V, Ju YM, Seip S, Henkel T (2007) Accelerated dereplication of natural products, supported by reference libraries. *Chimia* 51:332–338
- Bitzer J, Læssøe T, Fournier J, Kummer V, Decock C, Tichy HV, Piepenbring M, Persöh D, Stadler M (2008) Affinities of *Phylacia* and the daldinoid Xylariaceae, inferred from chemotypes of cultures and ribosomal DNA sequences. *Mycol Res* 112:251–270
- Fournier J, Köpcke B, Stadler M (2010a) New species of *Hypoxylon* from Western Europe and Ethiopia. *Mycotaxon* 113:209–235
- Fournier J, Stadler M, Hyde KD, Duong ML (2010b) The new genus *Rostrohypoxylon* and two new *Annulohypoxylon* species from Northern Thailand. *Fungal Divers* 40:23–36
- Gao JM, Yang SX, Qin JC (2013) Azaphilones: chemistry and biology. *Chem Rev* 113:4755–4811
- Halecker S, Surup F, Kuhnert E, Mohr KI, Brock NL, Dickschat JS, Junker C, Schulz B, Stadler M (2014) Hymenoseptin, a 3-decalinoyltetramic acid antibiotic from cultures of the ash dieback pathogen, *Hymenoscyphus pseudoalbidus*. *Phytochemistry* 100:86–91
- Hellwig V, Ju YM, Rogers JD, Fournier J, Stadler M (2005) Hypomiltin, a novel azaphilone from *Hypoxylon hypomiltum*, and chemotypes in *Hypoxylon* sect. *Hypoxylon* as inferred from analytical HPLC profiling. *Mycol. Progr.* 4:39–54
- Hsieh HM, Ju YM, Rogers JD (2005) Molecular phylogeny of *Hypoxylon* and closely related genera. *Mycologia* 97:844–865
- Ju YM, Rogers JD (1996) A revision of the genus *Hypoxylon*. *Mycologia* Memoir n° 20. APS Press, St. Paul, 365 pp
- Kuhnert E, Fournier J, Persöh D, Luangsa-ard JJ, Stadler M (2014a) New *Hypoxylon* species from Martinique and new evidence on the molecular phylogeny of *Hypoxylon* based on ITS rDNA and β -tubulin data. *Fungal Divers* 64:181–203
- Kuhnert E, Heitkämper S, Fournier J, Surup F, Stadler M (2014b) Hypoxyvermelhotins A–C, new pigments from *Hypoxylon lechatii* sp. nov. *Fungal Biol* 118:242–252
- Kuhnert E, Surup F, Sir EB, Lambert C, Hyde KD, Hladki AI, Romero AI, Stadler M (2015) Lenormandins A – G, new azaphilones from *Hypoxylon lenormandii* and *Hypoxylon jaklitschii* sp. nov., recognised by chemotaxonomic data. *Fungal Divers*, in press. doi: 10.1007/s13225-014-0318-1
- Læssøe T, Srikitikulchai P, Fournier J, Köpcke B, Stadler M (2010) Lepralic acid derivatives as chemotaxonomic markers in *Hypoxylon aeruginosum*, *Chlorostroma subcubisporum* and *C. cyaninum*, sp.nov. *Fungal Biol* 114:481–489
- Læssøe T, Srikitikulchai P, Luangsa-ard JJ, Stadler M (2013) *Theissenia* reconsidered, including molecular phylogeny of the type species *T. pyrenocrata* and a new genus *Durotheca* (Xylariaceae, Ascomycota). *IMA Fungus* 4:57–69
- Mühlbauer A, Triebel D, Persöh D, Wollweber H, Seip S, Stadler M (2002) Macrocarpones, novel metabolites from stromata of *Hypoxylon macrocarpum* and new evidence on the chemotaxonomy of *Hypoxylon*. *Mycol Prog* 1:235–248
- Okanya PW, Mohr KI, Gerth K, Jansen R, Müller R (2011) Marinoquinolines A – F, pyrroloquinolines from *Ohtaekwangia kribbensis* (Bacteroidetes). *J Nat Prod* 74:603–608
- Pažoutová S, Follert S, Bitzer J, Keck M, Surup F, Šrůtka P, Holuša J, Stadler M (2013) A new endophytic insect-associated *Daldinia* species, recognised from a comparison of secondary metabolite profiles and molecular phylogeny. *Fungal Divers* 60:107–123
- Quang DN, Hashimoto T, Stadler M, Asakawa Y (2004a) New azaphilones from the inedible mushroom *Hypoxylon rubiginosum*. *J Nat Prod* 67:1152–1155
- Quang DN, Hashimoto T, Tanaka M, Stadler M, Asakawa Y (2004b) Cyclic azaphilones daldinins E and F from the ascomycete fungus *Hypoxylon fuscum* (Xylariaceae). *Phytochemistry* 65:469–473
- Quang DN, Stadler M, Fournier J, Asakawa Y (2006) Carneic acids A and B, two chemotaxonomically significant antimicrobial agents

- from the xylariaceous ascomycete, *Hypoxylon carneum*. J Nat Prod 69:1198–1202
- Rayner RW (1970) A mycological colour chart. Commonwealth Mycological Institute, Kew and British Mycological Society
- Rogers JD (1981) Two new *Hypoxylon* species from Gabon. Can J Bot 59:1363–1364
- Rogers JD (2000) Thoughts and musings on tropical Xylariaceae. Mycol Res 104:1412–1420
- Singh SB, Kelly R, Guan Z, Polishook JD, Dombrowski AW, Collado J, González A, Pelaez F, Register E, Kelly TM, Bonfiglio C, Williamson JM (2006) New fungal metabolite geranyl-geranyltransferase inhibitors with antifungal activity. Nat Prod Res 19:739–747
- Stadler M, Fournier J (2006) Pigment chemistry, taxonomy and phylogeny of the Hypoxyloideae (Xylariaceae). Rev Iberoam Micol 23:160–170
- Stadler M, Fournier J, Læssøe T, Lechat C, Tichy HV, Piepenbring M (2008) Recognition of hypoxyloid and xylarioid *Entonaema* species from a comparison of holomorphic morphology, HPLC profiles, and ribosomal DNA sequences. Mycol Progr 7:53–73
- Stadler M, Ju YM, Rogers JD (2004) Chemotaxonomy of *Entonaema*, *Rhopalostroma* and other Xylariaceae. Mycol Res 108:239–256
- Stadler M, Kuhnert E, Persøh D, Fournier J (2013) The Xylariaceae as model for a unified nomenclature following the “One fungus-One Name” (1F1N) concept. Mycology 4:5–21
- Stadler M, Læssøe T, Fournier J, Decock C, Schmieschek B, Tichy HV, Peršoh D (2014) A polyphasic taxonomy of *Daldinia* (Xylariaceae). Stud Mycol 77:1–143
- Stadler M, Wollweber H, Mühlbauer A, Henkel T, Wollweber H, Asakawa Y, Hashimoto T, Rogers JD, Ju YM, Wetzstein HG, Tichy HV (2001) Secondary metabolite profiles, genetic fingerprints and taxonomy of *Daldinia* and allies. Mycotaxon 77:379–429
- Stamatakis A (2006) RAxML-VI-HPC: maximum likelihood-based phylogenetic analyses with thousands of taxa and mixed models. Bioinformatics 22:2688–2690
- Steglich W, Klaar M, Furtner W (1974) Mitorubrin derivatives from *Hypoxylon fragiforme*. Phytochemistry 13:2874–2875
- Surup F, Mohr KI, Jansen R, Stadler M (2013) Cohaerins G-K, azaphilone pigments from *Annulohypoxylon cohaerens* and absolute stereochemistry of cohaerins C-K. Phytochemistry 95:252–258
- Suwannasai N, Rodtong S, Thienhirun S, Whalley AJS (2005) New species and phylogenetic relationships of *Hypoxylon* species found in Thailand inferred from the internal transcribed spacer regions of ribosomal DNA sequences. Mycotaxon 94:303–324
- Suzuki S, Hosoe T, Nozawa K, Yaguchi T, Udagawa S, Kawai K (1999) Mitorubrin derivatives on ascomata of some *Talaromyces* species of ascomycetous fungi. J Nat Prod 62:1328–1329
- Triebel D, Peršoh D, Wollweber H, Stadler M (2005) Phylogenetic relationships among *Daldinia*, *Entonaema* and *Hypoxylon* as inferred from ITS nrDNA sequences. Nova Hedw 80:25–43
- Wang H, Wang Y, Wang W, Fu P, Liu P, Zhu W (2011) Anti-influenza virus polyketides from the acid-tolerant fungus *Penicillium purpurogenum* JS03-21. J Nat Prod 74:2014–2018